MARCH 1967 AIAA JOURNAL VOL. 5, NO. 3

Imperfection-Sensitivity of Eccentrically Stiffened Cylindrical Shells

JOHN W. HUTCHINSON* AND JOHN C. AMAZIGO†
Harvard University, Cambridge, Mass.

A quantitative study of the imperfection-sensitivity of eccentrically stiffened cylindrical shells is presented. Results are given for both axial and ring stiffened cylinders under axial compression and hydrostatic pressure. In some instances, in particular in the case of axially stiffened cylinders under axial load, the sensitivity to imperfections, as well as the classical buckling load, appears to be strongly dependent on whether the stringers are attached to the outside or inside of the cylinder. Under certain conditions stiffening can significantly reduce or perhaps completely eliminate imperfection-sensitivity, whereas in other cases it may play a much smaller role in lowering the sensitivity.

Nomenclature

a = postbuckling coefficient; see Eq. (25)
A_{xx}, A_{xy}, A_{yy} = see Table 1
A_r, A_s = cross-sectional area of ring and stiffener
$B_{xx}, \bar{B}_{xx}$, etc. = see Table 1
b = postbuckling coefficient; see Eq. (1)
C = $[3(1-\nu^2)]^{1/2}$
D = $Et^3/12(1-\nu^2)$
$D_{xx}, \bar{D}_{xx}$, etc. = effective bending stiffnesses; see Table 1
$D(\ ,\ )$ = see Eq. (30)
d_r, d_s = ring and stringer spacing; see Fig. 2
E = Young's modulus
e_r, e_s = ring and stringer eccentricity; see Fig. 2
F = stress function
$F^0, F^{(1)}, F^{(2)}$ = see Eq. (22)
$\bar{F}$ = see Eq. (29)
$H_{xx}, \bar{H}_{xx}$, etc. = effective stretching stiffnesses; see Table 1
$H(\ ,\ )$ = see Eq. (30)
I_r, I_s = ring and stringer moment of inertia
L = cylinder length
L_D, L_H, L_Q = differential operators defined in Eq. (17)
l = axial wavelength of buckle pattern; see Eq. (9)
M_r, M_s = ring and stringer bending moment
M_x, M_y, M_{xy} = bending moment in shell; not in composite shell
m = number of axial half-wavelengths
N_r = $\sigma_r A_r/d_r$
N_s = $\sigma_s A_s/d_s$
N_x, N_y, N_{xy} = resultant membrane stresses in shell; see Eq. (13)
N_x^0, N_s^0, etc. = prebuckling reference stresses; see Eq. (20)
$\bar{N}_x^0, \bar{N}_y^0, \bar{N}_r^0, \bar{N}_s^0$ = $CR/Et^2 \times (N_x^0, N_y^0, N_r^0, N_s^0)$
n = number of circumferential wavelengths in buckle pattern
$\bar{n}$ = $nL/\pi R$
P = compressive axial load
P_C = classical buckling load
P_S = buckling (maximum) load of imperfect cylinder

Received May 5, 1966; revision received October 3, 1966. This work was supported in part by NASA under Grant NsG-559, and by the Division of Engineering and Applied Physics, Harvard University.

* Assistant Professor of Structural Mechanics, Division of Engineering and Applied Physics.
† Graduate Student, Division of Engineering and Applied Physics.

$(P_C)_{unstiff}$ = $2\pi[3(1-\nu^2)]^{-1/2}Et^2$ (classical buckling load of long unstiffened cylinder)
P^0, p^0 = prebuckling reference values; see Eq. (20)
p_C = classical buckling pressure
p_S = buckling pressure of imperfect cylinder
Q_{xx}, $\bar{Q}_{xx}$, etc. = see Table 1
$Q_{(\ ,\ )}$ = see Eq. (30)
R = cylinder radius
t = shell thickness; not effective thickness
U = axial displacement of shell middle surface
V = circumferential displacement
W = normal displacement
$\bar{W}$ = initial displacement of unloaded shell (imperfection)
$W^{(1)}$, $W^{(2)}$ = see Eq. (22)
x = axial coordinate
y = circumferential coordinate
Z = $(L^2/Rt)(1-\nu^2)^{1/2}$
$\bar{Z}$ = $2\,3^{1/2}Z/\pi^2$
α_i, β_i, γ_i, ζ_i = defined in Equation (31)
ϵ_r, ϵ_s = strain at the neutral axis of ring and stringer
ϵ_x, ϵ_y, ϵ_{xy} = membrane strains in shell
δ = buckling displacement amplitude
$\bar{\delta}$ = initial displacement amplitude (imperfection)
K_x, K_y, K_{xy} = bending strains in shell
λ = scalar load parameter
λ_C = classical value of scalar load parameter
λ_S = maximum value of scalar load parameter for imperfect structure
ν = Poisson's ratio
σ_r, σ_s = $E\epsilon_r$, $E\epsilon_s$

Introduction

As early as 1947, van der Neut[1] observed that the buckling load of an axially compressed cylindrical shell with stiffeners attached to the outside can be two or even three times the buckling load of a cylinder that is identical in all respects, except that the stiffeners are attached to the inside. Apparently, the potential of this remarkable effect remained more or less unappreciated until interest was revived by Hedgepeth and Hall,[2] who made a fairly extensive study of eccentricity effects on axial buckling, and by Baruch and Singer,[3] who investigated buckling of eccentrically stiffened cylindrical shells under hydrostatic pressure. These and subsequent studies were based on linear buckling equations and, therefore, will be described herein as classical buckling analyses. Tests have provided experimental verification of the advantage of outside over inside stiffening for the case of axial buckling. Moreover, some test results are in fair agreement with the predictions of the classical buckling theory. This, of course, is in marked contrast to the buckling behavior of unstiffened cylinders under axial compression which often buckle at a small fraction of the classical buckling load. It has been suggested that the classical buckling analysis should be adequate to predict the buckling loads of stiffened cylinders by virtue of the fact that stiffening increases the effective thickness of the shell and thus, so the argument goes, reduces the susceptibility of the shell to small imperfections.

This paper presents a quantitative study of the imperfection-sensitivity of eccentrically stiffened cylindrical shells under both axial and hydrostatic loadings. For the most part, the investigation is made within the framework of Koiter's general theory of postbuckling behavior.[4–6] The calculations provide a measure of the extent to which the shells are sensitive or insensitive to imperfections in their shape and thus indicate to what extent the classical buckling results can be considered reliable.

Buckling of Imperfection-Sensitive Shells

Koiter has shown that the imperfection-sensitivity of a structure is closely related to its initial postbuckling behavior.

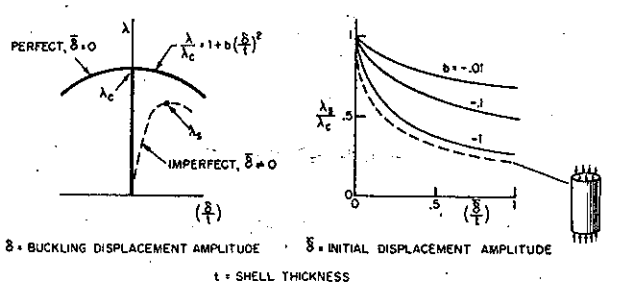

Fig. 1 Buckling of imperfection-sensitive shells.

In nearly all the circumstances encountered in this paper, the shell structures are characterized by a unique buckling mode associated with the classical buckling load, and their buckling and initial postbuckling behavior can be represented fairly simply in the manner pictured in Fig. 1. The perfect shell suffers no buckling deformation until the classical buckling load λ_C is reached. If, as pictured on the left in Fig. 1, the bifurcation point is symmetric with respect to the buckling deflections, then the initial postbuckling behavior is governed by the equation

$$\lambda/\lambda_C = 1 + b(\delta/t)^2 \qquad (1)$$

where λ is the applied load, which will be identified with either the axial load P or the hydrostatic pressure p. The amplitude of the buckling displacement normal to the shell δ has been normalized with respect to the shell thickness t. When b is *negative*, the equilibrium load *falls* following buckling, and this is the case shown in Fig. 1. Under dead loading, such behavior is often associated with catastrophic buckling. On the other hand, if b turns out to be positive, initially at least, the perfect structure can support loads in excess of the classical load.

A structure can be expected to be imperfection-sensitive if its postbuckling coefficient b is negative. In this study imperfections are assumed to be initial deviations of the shell middle surface from the perfect cylindrical configuration and these initial deflections are taken in the shape of the normal buckling displacement. Koiter has shown that the buckling load of the imperfect shell λ_S (the maximum load the structure can support prior to buckling) is related to the imperfection amplitude $\bar{\delta}$ and the postbuckling coefficient b by

$$\left(1-\frac{\lambda_S}{\lambda_C}\right)^{3/2} = \frac{3\,(3)^{1/2}}{2}(-b)^{1/2}\left|\frac{\bar{\delta}}{t}\right|\frac{\lambda_S}{\lambda_C} \qquad b<0 \qquad (2)$$

This equation is asymptotically valid for small imperfections. Curves displaying the ratio of the buckling load to the classical load λ_S/λ_C as a function of the imperfection amplitude $\bar{\delta}$ are given on the right in Fig. 1. These curves are intended to serve as reference for the calculated postbuckling coefficients presented in later parts of the paper. It should be emphasized that the imperfection amplitude $\bar{\delta}$ has been normalized with respect to the shell thickness t and not some effective thickness of the stringer-shell combination. Included in this series of curves is a plot, taken from Koiter,[5] showing the effect of axisymmetric imperfections on the buckling load of an unstiffened cylindrical shell under axial compression. Although the monocoque cylinder under axial compression is not characterized by Eqs. (1) and (2), the curve does provide a calibration for the role of the postbuckling coefficient b in the case of structures that have just one buckling mode associated with a symmetric bifurcation point. Circumstances arise in which the characterization provided by Eqs. (1) and (2) does not permit an adequate assessment of imperfection-sensitivity. These cases will be discussed and analyzed by alternative methods as they are encountered.

The shell configurations are shown in Fig. 2. Only general instability of the cylinders is considered here and all calculations are based on "smeared-out" stringer and ring proper-

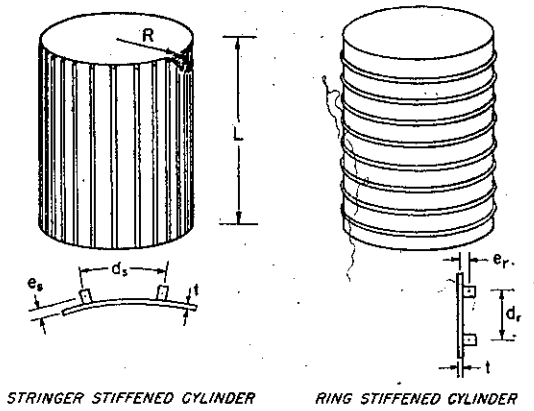

Fig. 2 Stiffened shell configurations.

ties. The governing equations, whose derivation is given in the Appendix, are based on nonlinear Donnell-type strain-displacement relations. In their final form, the equations have been reduced to two equations, an equilibrium equation and a compatibility equation, involving the normal displacement and a stress function. Details of the classical and postbuckling analyses are given in the Appendix, whereas the results of these calculations are presented and discussed in the following sections. The results presented are in every case for simply supported cylinders. To simplify the calculations involved, the prebuckling displacements are neglected as is customary, especially in preliminary or exploratory studies such as this. It should be mentioned that no attempt has been made to uncover optimum stiffening conditions; rather, the effect of imperfections on the buckling loads of quite a wide range of stiffening possibilities has been studied.

Axially Stiffened Cylinders under Axial Compression

Classical buckling studies of eccentrically stiffened cylindrical shells under axial compression have been reported in Refs. 1, 2, and 7–9. A comprehensive parameter study is contained in Ref. 8. Plots of the classical buckling loads of lightly, moderately, and heavily stiffened cylinders are given in Fig. 3. The relative strengthening capabilities of outside and inside stiffening are evident. In the present formulation the axial stiffening is characterized by three dimensionless parameters A_s/d_st, EI_s/Dd_s, and e_s/t, where A_s is the area of the stringer cross-section, I_s is the stringer moment of inertia about its neutral axis, and e_s, the stringer eccentricity, is positive for outside stiffening and negative for inside stiffening. The torsional stiffness and lateral (tangent to shell) bending stiffness are not taken into account.

The postbuckling coefficient b is plotted just beneath the classical buckling curves in Fig. 3. Since imperfection-sensitivity is associated with negative values of b (refer back to Fig. 1), it would appear that even heavily stiffened cylinders may be susceptible to initial deflections, which are of the order of the shell thickness. As previously indicated, the imperfection is assumed to be in the shape of the buckling mode, i.e.,

$$\bar{W} = \bar{\delta} \sin(m\pi x/L) \cos(ny/R) \qquad (3)$$

The major conclusion to be drawn from the results of Fig. 3 is that an outside-stiffened cylinder is generally more imperfection-sensitive than one with inside stiffening, and its buckling load may be appreciably below the classical buckling load. Thus, without further evidence, either theoretical or experimental, it would be a mistake not to take a suspicious view of the quantitative predictions of the classical analysis, particularly with regard to the advantage of outside over inside stiffening.

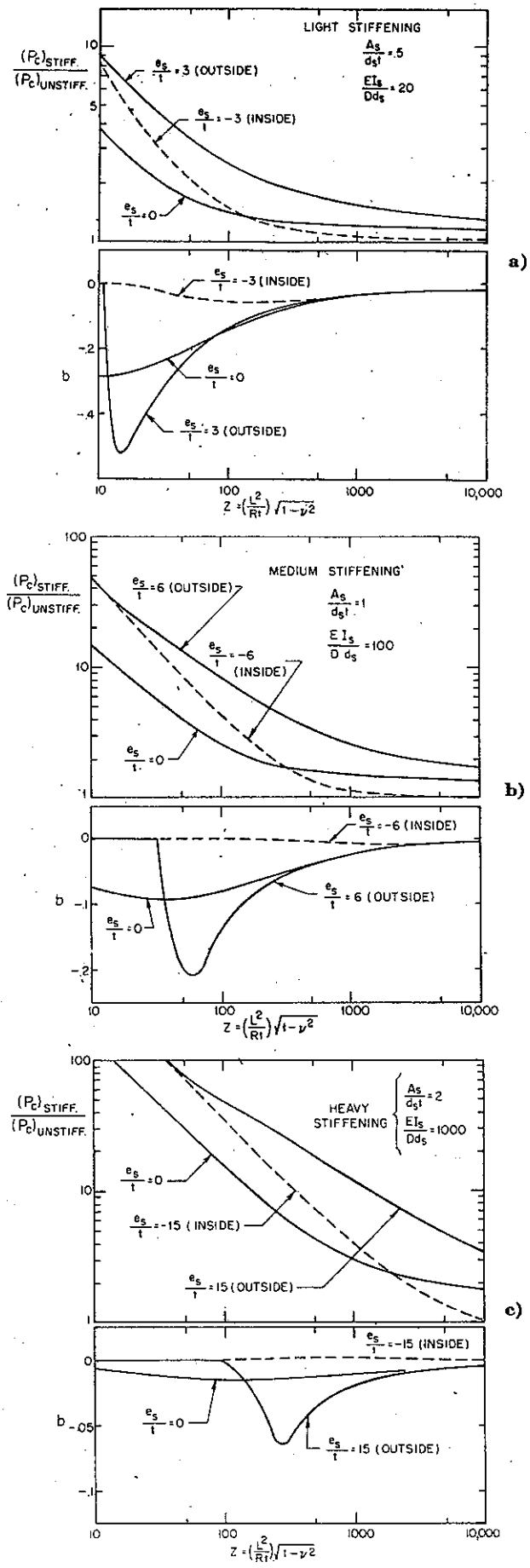

Fig. 3 Classical buckling and imperfection-sensitivity of simply supported, axially stiffened cylinders under axial compression.

For all values of Z less than a certain value, an externally stiffened cylinder buckles axisymmetrically. Usually, except for a heavily stiffened cylinder such as that discussed below, axisymmetric buckling occurs at too low a value of Z to be of practical interest. However, when this does occur, the postbuckling coefficient is identically zero. The transition to axisymmetric buckling is marked by the discontinuity in slope of the curve of b vs Z at the point where b becomes zero. A schematic sketch of the load-buckling deflection behavior for the case of an axisymmetric classical buckling mode is shown on the left in Fig. 4. Once the classical buckling load P_C is attained the perfect cylinder deflects in its axisymmetric buckling mode under constant load until bifurcation from the axisymmetric state of deformation occurs. Following bifurcation, the load falls below P_C with increasing axisymmetric and nonaxisymmetric deflections. Calculations have been carried out to determine the effect of an imperfection in the shape of the axisymmetric buckling mode

$$\bar{W} = -\bar{\delta} \sin(\pi x/L) \tag{4}$$

on the bifurcation load P_S marking the first occurrence of nonaxisymmetric deflections. The curve of load vs buckling deflection is depicted as falling following bifurcation. This is only a conjecture. In any case, P_S is probably the most meaningful measure of the buckling strength of the imperfect cylinder. Curves of P_S/P_C vs $\bar{\delta}/t$ are shown on the right in Fig. 4 for the heavily stiffened cylinder. With diminishing Z, the buckling behavior of the cylinder becomes more and more like that of a wide column; and as reflected in the trends of Fig. 4, the cylinder becomes less and less imperfection-sensitive. It should be mentioned that the calculation of the bifurcation load P_S is approximate but, as discussed in the Appendix, the prediction for a given imperfection amplitude is an upper bound to the actual bifurcation load.

To date, the limited number of tests which have been performed have more or less verified the beneficial strengthening effect of outside stiffening. The test loads of Card's[10] cylinders were from 70 to 95% of the classical values.[11] This is not surprising since each cylinder tested was associated with large values of Z out of the range in which b is most negative and out of the range in which an outside-stiffened cylinder should be anymore imperfection-sensitive than one with inside-stiffening. Card's[10] cylinders, for example, roughly corresponded to the medium stiffened cylinders of Fig. 3 (they were clamped at the ends, not simply supported) and none of the specimens had a Z less than 1000. The present results, then, indicate a critical imperfection-sensitive range for outside stiffened cylinders under axial compression; and as far as the writers are aware, no tests have been performed which would reveal just how critical imperfections are in this range of Z. These considerations may be important, for example, in arriving at the design load of an externally stiffened cylinder which was recently investigated[2] as a possible structure for a post-Saturn vehicle. This

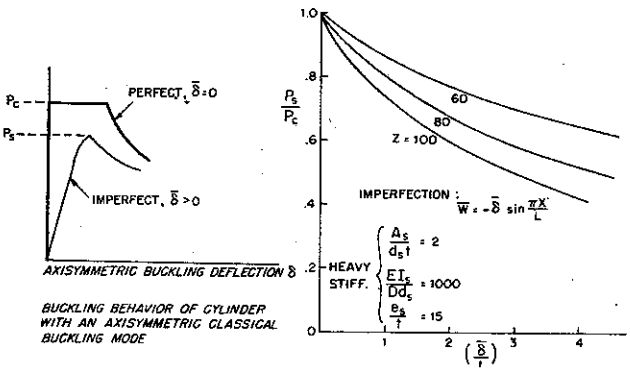

Fig. 4 Effect of axisymmetric imperfections on axially compressed cylinders with outside axial stiffeners.

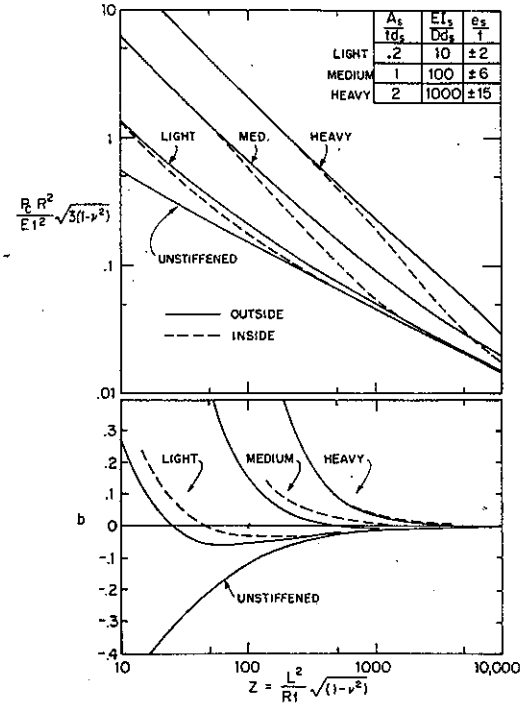

Fig. 5 Classical buckling and imperfection-sensitivity of simply supported, axially stiffened cylinders under hydrostatic pressure.

structure does fall in the critical range ($A_s/dt = 0.94$, $e_s/t = 34$, $EI_s/Dd_s = 765$, $Z = 66.5$ and $b = -0.05$).

Finally, a remark concerning the interpretation of postbuckling calculations of the large deflection type seems called for. Imperfection-sensitivity predictions, based on finite deflection calculations, and in particular on the minimum support load of a perfect cylinder in the postbuckling region, would imply that imperfection sensitivity grows with increasing Z. In fact, the minimum support load of a long axially stiffened cylinder is only slightly different from that of a monocoque cylinder [see Almroth's calculations for orthotropic cylinders ($e_s = 0$) under axial compression[12]]. This runs counter to the predictions of the initial postbuckling analysis which indicate that an orthotropic cylinder is most susceptible to small imperfections in an intermediate range of Z. How susceptible they are in the critical range remains to be seen. However, the fact that test loads are in fair agreement with the classical predictions for large values of Z points to the initial post-buckling coefficient b as being a better measure of imperfection-sensitivity than the minimum support load.

Axially Stiffened Cylinders under Hydrostatic Pressure

Figure 5 displays the classical buckling pressure and postbuckling coefficient of stiffened and unstiffened cylindrical shells under hydrostatic loading. The classical buckling pressure of the unstiffened cylinder is that calculated by Batdorf[13] (a different buckling parameter has been used here) and the associated post-buckling coefficient was given in Ref. 14. Tests[15] bear out the predicted sensitivity of the unstiffened cylinders in the range roughly corresponding to $Z < 100$, with occurrence of test buckling pressures that are as low as one half the classical values.

The major effect of axial stiffening is to eliminate imperfection-sensitivity in the lower range of Z. Even very light stiffening significantly diminishes the postbuckling coefficient in the range of Z in which unstiffened cylinders are most sensitive. When the postbuckling coefficient is positive, in all likelihood, buckling will not be accompanied by

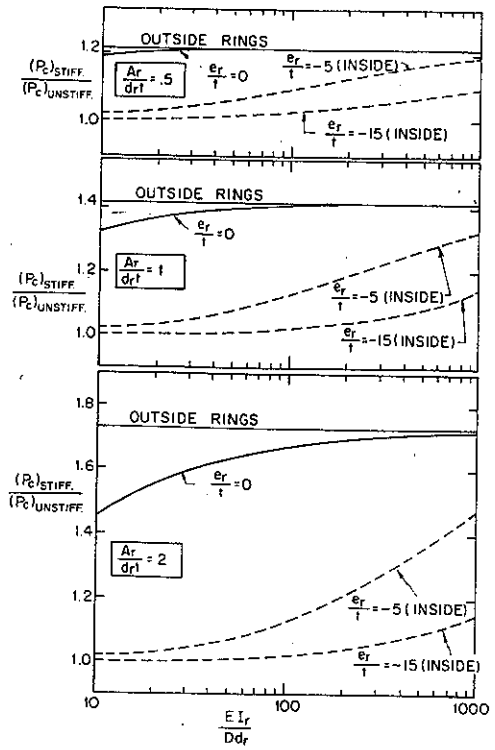

Fig. 6 Classical buckling of "long" ring stiffened cylinders under axial compression.

catastrophic collapse and the cylinder may be able to sustain pressures above the classical buckling pressure. The inside-outside effect of stiffening is less prominent in buckling under hydrostatic pressure than under axial compression. Over some of the range of Z, however, there is a definite advantage in outside stiffening. At the same time, the postbuckling coefficient b provides a hint, but little more, that an outside-stiffened cylinder may be more sensitive to imperfections than its inside-stiffened counterpart. Out of all this, the most important result is that the classical buckling load should be a reliable index of buckling strength in the lower range of Z. It will be seen later that this may indicate a clear preference in certain circumstances for increasing the buckling strength by employing axial stiffening rather than ring stiffening.

Ring Stiffened Cylinders under Axial Compression

In some respects, this is the least interesting of the stiffening-loading cases studied in this paper. Only if the value of Z is very large can the classical buckling load of a ring stiffened cylinder under axial compression exceed that of a cylinder with an equivalent amount of axial stiffening. The major point to be established is that small imperfections can be expected to reduce the buckling load of both outside and inside stiffened cylinders well below the classical buckling load. The parameters characterizing ring stiffening properties are analogous to those for axial stiffening, namely, $A_r/d_r t$, EI_r/Dd_r, and e_r/t.

The dependence of the classical buckling load on eccentricity and stiffening is shown in Fig. 6 for "long" cylinders. A long cylinder is taken to be any cylinder longer than several axial wavelengths of the buckle pattern so that the buckling load and wavelength are essentially independent of the cylinder length and Z. An outside-stiffened cylinder with sufficient eccentricity has an axisymmetric buckling mode with a (short) axial wavelength

$$l = 2\pi(Rt)^{1/2}[12(1 - \nu^2)(1 + A_r/d_r t)]^{-1/4} \tag{5}$$

and classical buckling load given by

$$\frac{(P_c)_{stiff}}{(P_c)_{unstiff}} = \left[1 + \frac{A_r}{d_r t}\right]^{1/2} \tag{6}$$

independent of I_r and e_r.‡ If there is no eccentricity or internal rings, the buckling mode is not axisymmetric but it does have an axial wavelength which is almost as short as given by Eq. (5). When nonaxisymmetric buckling takes place, the classical buckling load depends on both the eccentricity and bending stiffness of the rings as shown in Fig. 6. The advantage of outside to inside rings is also apparent.

Consider first the effect of imperfections on an externally stiffened cylinder. When the classical buckling mode is axisymmetric, as it is when the rings are on the outside of the cylinder, the perfect cylinder can continue to deform in its buckling mode under constant load once the classical buckling load P_c has been attained and, therefore, b is identically zero. Purely axisymmetric deformations persist until bifurcation from the axisymmetric deformation state results in a branch of the equilibrium curve on which the applied load falls with increasing deflections, as depicted in Fig. 7. Imperfections in the shape of the classical buckling mode

$$\bar{W} = \bar{\delta} \sin(2\pi x/l) \tag{7}$$

reduce the axial load P_s at which nonaxisymmetric deformations first occur. This behavior and the calculated values of P_s/P_c vs $\bar{\delta}/t$ are shown in Fig. 7. For purposes of comparison, the bifurcation curve for an unstiffened cylinder with an axisymmetric imperfection, taken from Koiter,[16] is also given in this figure. Although the estimate of P_s is approximate, it is an upper bound, as discussed in the Appendix.

Finite-deflection load-end-shortening curves for initially perfect ring stiffened orthotropic cylinders with no eccentricity have been calculated by Thielemann.[17] Following buckling the support load increases a small amount above the classical buckling load with deflection occurring mainly in the (nonaxisymmetric) classical buckling mode. When the load is large enough (but still only slightly greater than P_c) deflections in modes other than the classical buckling mode become important and then the support load falls. In the present study, the initial postbuckling coefficient b was calculated and found to be positive for the cases of both internal rings and no eccentricity. Thus, Thielemann's result that following buckling the perfect cylinder can support loads which are slightly in excess of P_c is confirmed by the present exact initial post-buckling calculations. We are dealing, then, with a structure, which appears to be relatively insensitive

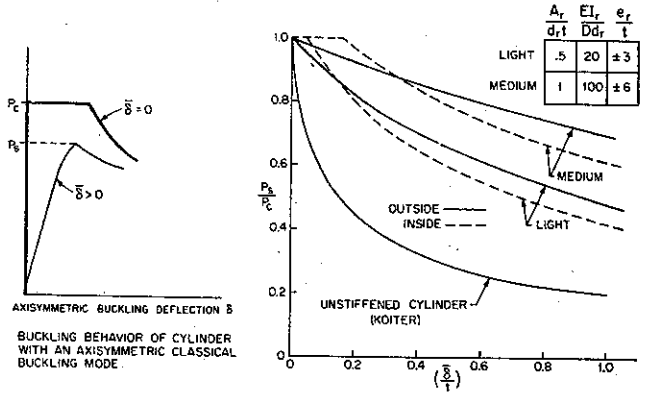

Fig. 7 Effect of axisymmetric imperfections on axial buckling of ring stiffened cylinders.

‡ The shortness of the axial wavelength places rather severe limitations on the applicability of the present results which were derived using "smeared-out" stiffening properties—a technique that only applies when the buckle wavelength is large compared to the spacing between rings.

to imperfections in the shape of the classical buckling mode. On the other hand, it will be shown that it is sensitive to imperfections of other shapes. A complete study has not been made and, in fact, we will content ourselves with demonstrating that a particular axisymmetric imperfection, given by Eq. (7), results in quite large buckling load reductions.

Curves of P_S/P_C vs $\bar{\delta}/t$ for two cases of inside stiffening are shown in Fig. 7, together with the curves for the corresponding outside-stiffened cylinders. Here, P_S is, again, the load at which bifurcation from the axisymmetric state of deformation occurs and P_C is the classical buckling load of the internally stiffened cylinder. Note that no reduction in the buckling load takes place for very small $\bar{\delta}$ because there is essentially no interaction between the imperfection-induced deflections and the nonaxisymmetric classical buckling mode. For larger values of $\bar{\delta}$, P_S is below P_C and is associated with bifurcation into a nonaxisymmetric mode, which is not the classical buckling mode. On the basis of just this limited number of results, it does seem reasonable to expect that ring stiffened cylindrical shells may buckle at axial loads, which are well below the classical buckling load.

Ring Stiffened Cylinders under Hydrostatic Pressure

The general classical buckling behavior and imperfection-sensitivity of ring stiffened cylinders under hydrostatic pressure is more complex than the load-stiffening combinations studied in the previous sections. Baruch, Singer and Harari[18] have carried out the most extensive classical buckling study to date. The classical buckling pressure and postbuckling coefficient of a lightly stiffened cylinder can be compared with the corresponding quantities for an unstiffened cylinder in Fig. 8. In the lower range of Z the classical buckling load is higher if the rings are attached to the outside whereas the opposite occurs for larger values of Z. Judging from the postbuckling coefficient it would appear that the inside-stiffened cylinder is slightly less imperfection-sensitive in the lower range of Z than an outside-stiffened cylinder, although this effect is not sufficiently pronounced to warrant any general conclusions.

The lightly stiffened cylinder just discussed buckles into a mode that has only one half-wavelength over the length of the cylinder. If the amount of stiffening is increased the number of axial half-wavelengths in the classical buckle pattern will not necessarily be one and, in fact, may be very large depending on the stiffening and the value of Z. Classical buckling loads for three other degrees of stiffening are shown in Fig. 9. In the range in which the buckling parameter is independent of Z, the buckling load is determined mainly by the axial component of the hydrostatic pressure in much the same way as discussed in the previous section, and the axial wavelength is very short. The classical buckling mode of an outside-stiffened cylinder is axisymmetric in the Z independent range and the classical buckling pressure is

$$[3(1-\nu^2)]^{1/2}\frac{p_c}{E}\left(\frac{R}{t}\right)^2 = 2\left(1+\frac{A_r}{d_r t}\right)^{1/2} \qquad (8)$$

independent of the ring bending stiffness; and the axial wavelength of the buckle pattern is the same as in the axial compression case

$$l = 2\pi(Rt)^{1/2}[12(1-\nu^2)(1+A_r/d_r t)]^{-1/4} \qquad (9)$$

With rings on the inside, the buckle pattern is not axisymmetric but it does have an axial wavelength that is not much longer than that given by (9). In the Z-dependent range, the cylinder buckles into a nonaxisymmetric mode with, again, only one half-wavelength over the axial length of the shell.

The postbuckling coefficient b in the Z-dependent range follows the trends noted in Fig. 8, namely, the magnitude of b decreases with increasing stiffness but its sign remains negative. In the Z-independent range, the postbuckling behavior is similar to that of a ring stiffened cylinder under axial compression. The cases of outside and inside rings are discussed in turn.

When the classical buckling mode is axisymmetric the perfect cylinder deforms axisymmetrically under constant pressure p_C until bifurcation from the axisymmetric state occurs and subsequently the load falls. Imperfections in the shape of the buckling mode

$$\bar{W} = \bar{\delta}\sin(2\pi x/l)$$

reduce the pressure p_S at which bifurcation from the axisymmetric state takes place. Curves of p_S/p_C vs $\bar{\delta}/t$ for several degrees of stiffening are shown in Fig. 10.

Next, the effect of this same imperfection on internally stiffened cylinders can also be seen in Fig. 10. The comments made in the last section are relevant here as well. On the basis of the initial postbuckling analysis, it would appear that the cylinders are less susceptible to an imperfection in the shape of the nonaxisymmetric classical buckling mode than to imperfections in other shapes.

The results presented here fall short of providing anywhere near a complete picture of the initial postbuckling behavior of ring stiffened cylinders in the Z independent range. On the other hand, it does seem reasonable to conclude that

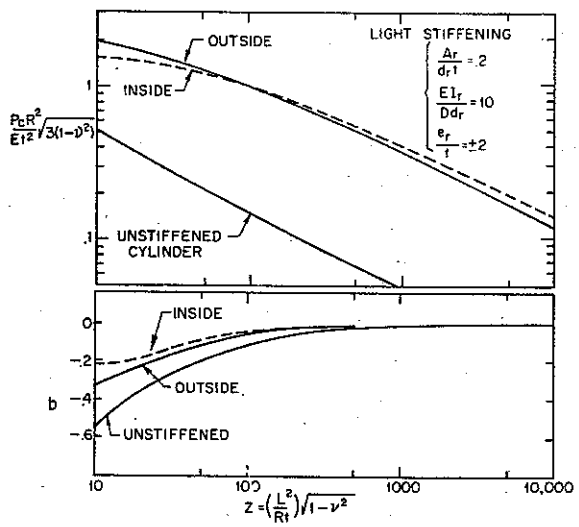

Fig. 8 Classical buckling and imperfection-sensitivity of simply supported, ring stiffened cylinders under hydrostatic pressure.

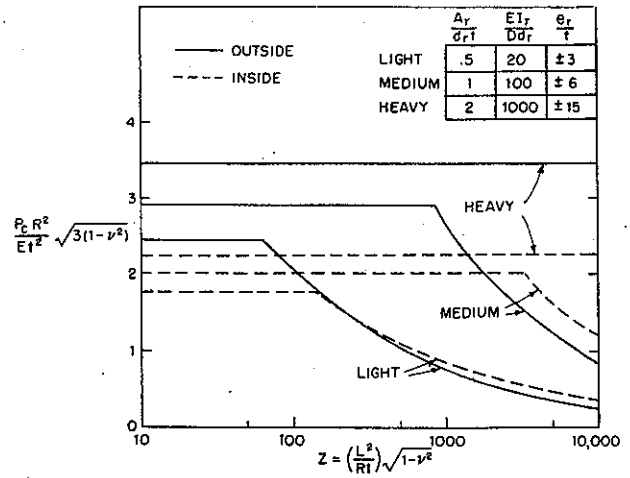

Fig. 9 Classical buckling of simply supported, ring stiffened cylinders under hydrostatic pressure.

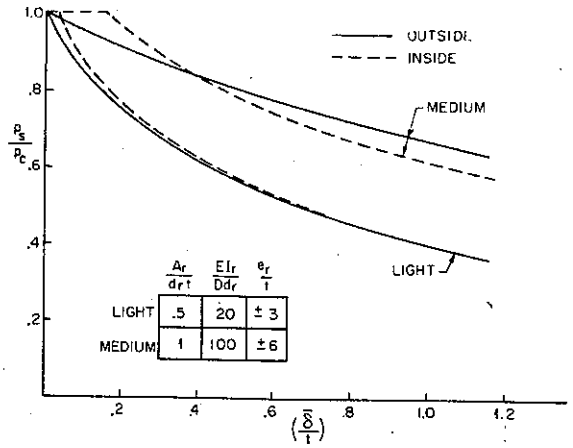

Fig. 10 Effect of axisymmetric imperfections on hydrostatic buckling of ring stiffened cylinders in the Z-independent range.

imperfections may result in fairly drastic buckling load reductions.

Under certain circumstances, axial stiffening may be a more efficient means of strengthening against buckling under hydrostatic pressure than ring stiffening. Comparing the results of Figs. 5 and 9, one notes that an axially stiffened cylinder can have a higher classical buckling pressure than a cylinder with an equivalent amount of ring stiffening. If, in addition, one takes into account the predicted insensitivity of the axially stiffened cylinder in the lower range of Z and the sensitivity of the ring stiffened specimens, then the advantage of axial stiffening is even more pronounced. Probably, an optimum choice would lead to a combination of axial and ring stiffening.

Appendix: Formulation of Equations and Postbuckling Calculations

Nonlinear Equations for Eccentrically Stiffened Cylindrical Shells

Let the two tangential and normal displacements of the shell middle surface be denoted by U, V, and W. Then according to Donnell-type theory the middle surface strains in the shell are

$$\epsilon_x = U_{,x} + \tfrac{1}{2}W_{,x}^2 \qquad \epsilon_y = V_{,y} + W/R + \tfrac{1}{2}W_{,y}^2$$
$$\epsilon_{xy} = \tfrac{1}{2}(U_{,y} + V_{,x}) + \tfrac{1}{2}W_{,x}W_{,y} \tag{10}$$

and the bending strains are given by $K_x = -W_{,xx}$, $K_y = -W_{,yy}$ and $K_{xy} = -W_{,xy}$. The axial strain at the neutral axis of an axial stringer attached to the shell surface is

$$\epsilon_s = \epsilon_x - e_s W_{,xx} \tag{11}$$

where e_s is the distance from the neutral axis of the stringer to the middle surface of the shell—positive if the stringer is located on the outside and negative if on the inside. The bending strain in the stringer is taken to be the same as in the shell, $-W_{,xx}$. The torsional stiffness and lateral bending stiffness of the stringer are neglected in this formulation. Similarly, the strain at the neutral axis of a ring stiffener is

$$\epsilon_r = \epsilon_y - e_r W_{,yy} \tag{12}$$

and the bending strain is $-W_{,yy}$. The bending and stretching stresses are related to the strain quantities in the usual manner, i.e., $\epsilon_x = (1/Et)(N_x - \nu N_y)$, $\epsilon_s = \sigma_s/E$, $\epsilon_r = \sigma_r/E$, $M_x = D(K_x + \nu K_y)$, $M_s = -EI_s W_{,xx}$, $M_r = -EI_r W_{,yy}$, etc.

Equilibrium equations are now obtained via the principle of virtual work. In formulating this principle the stringers and rings are "smeared-out" to arrive at equation governing the general instability of a shell. Thus, the force in a discrete stringer is replaced by an effective contribution N_s to the resultant membrane stress so that $N_s = \sigma_s A_s/d_s$ and also $N_r = \sigma_r A_r/d_r$. With the aid of the calculus of variations, the principle of virtual work leads to three equilibrium equations and associated boundary conditions. Next, a stress function is introduced such that the two inplane equilibrium equations are satisfied identically. The total stress resultants are related to the stress function by

$$N_x + N_s = F_{,yy} \qquad N_y + N_r = F_{,xx}$$
$$N_{xy} = -F_{,xy} \tag{13}$$

In this way the three equilibrium equations are reduced to a single equilibrium equation and a compatibility equation

$$\epsilon_{x,\,yy} + \epsilon_{y,\,xx} - 2\epsilon_{xy,\,xy} = W_{,xy}^2 - W_{,xx}W_{,yy} + W_{,xx}/R \tag{14}$$

When written in terms of W and F, these two equations are just a generalized form of the von Karman-Donnell equations appropriate for eccentrically stiffened cylindrical shells. These equations are

$$L_D[W] + L_Q[F] = F_{,xx}W_{,yy} + F_{,yy}W_{,xx} - 2F_{,xy}W_{,xy} + p \tag{15}$$

$$L_H[F] - L_Q[W] = W_{,xy}^2 - W_{,xx}W_{,yy} \tag{16}$$

where the differential operators are defined by

$$L_D[\ ] = D_{xx}[\ ]_{,xxxx} + 2D_{xy}[\ ]_{,xxyy} + D_{yy}[\ ]_{,yyyy}$$
$$L_Q[\ ] = Q_{xx}[\ ]_{,xxxx} + 2Q_{xy}[\ ]_{,xyxy} + Q_{yy}[\ ]_{,yyyy} + (1/R)[\ ]_{,xx} \tag{17}$$
$$L_H[\ ] = H_{xx}[\ ]_{,xxxx} + 2H_{xy}[\ ]_{,xxyy} + H_{yy}[\ ]_{,yyyy}$$

and where the effective bending and stretching stiffnesses and eccentricity coupling terms are given in Table 1.§ The resultant membrane stresses in the shell can also be written in terms of W and F:

$$N_x = F_{,yy} - N_s = A_{xx}F_{,xx} + A_{xy}F_{,yy} + B_{xx}W_{,xx} + B_{xy}W_{,yy}$$
$$N_y = F_{,xx} - N_r = A_{yy}F_{,yy} + A_{yx}F_{,xx} + B_{yy}W_{,yy} + B_{yx}W_{,xx} \tag{18}$$

where the coefficients appearing in these equations are also defined in Table 1. The tangential displacements must be single-valued over any complete circuit of the shell. For the circumferential displacement this condition is enforced if

$$\int_0^{2\pi R}\left[\frac{1}{Et}(N_y - \nu N_x) - \frac{W}{R} - \frac{1}{2}W_{,y}^2\right]dy = 0 \tag{19}$$

Classical Buckling and Initial Postbuckling Calculations

If the perfect cylinder is subject to an external hydrostatic pressure λp^0 plus an axial load per unit length $\lambda P^0/2\pi R$ applied through the effective centroid of the stiffened shell, then the prebuckling stresses are linearly related to the scalar load parameter λ by

$$\lambda(N_x^0 + N_s^0) = \lambda F_{,yy}^0 = -\lambda(P^0/2\pi R + p^0 R/2)$$
$$\lambda(N_y^0 + N_r^0) = \lambda F_{,xx}^0 = -\lambda p^0 R \tag{20}$$

§ If the initial displacement from the perfect cylindrical configuration is $\bar{W}(x, y)$, the equations are amended by adding the term $F_{,xx}\bar{W}_{,yy} + F_{,yy}\bar{W}_{,xx} - 2F_{,xy}\bar{W}_{,xy}$ to the right-hand side of Eq. (15) and $-\bar{W}_{,xx}W_{,yy} - \bar{W}_{,yy}W_{,xx} + 2\bar{W}_{,xy}W_{,xy}$ to the right-hand side of Eq. (16). A parallel derivation of Eqs. (15–17) has been given by Geier.[19]

Table 1 Stiffened cylinder parameters[a]

$$A_{xx} = \nu\alpha_s/\alpha_0 \qquad A_{yy} = \nu\alpha_r/\alpha_0 \qquad A_{xy} = (1+\alpha_r)/\alpha_0 \qquad A_{yx} = (1+\alpha_s)/\alpha_0$$

$$\bar{B}_{xx} = \alpha_s\gamma_s(1+\alpha_r)/\alpha_0 \qquad \bar{B}_{yy} = \alpha_r\gamma_r(1+\alpha_s)/\alpha_0 \qquad \bar{B}_{xy} = \nu\alpha_s\alpha_r\gamma_r/\alpha_0 \qquad \bar{B}_{yx} = \nu\alpha_r\alpha_s\gamma_s/\alpha_0$$

$$\bar{D}_{xx} = 1 + \beta_s + [12(1-\nu^2)\alpha_s(1+\alpha_r)\gamma_s^2]/\alpha_0 \qquad \bar{D}_{yy} = 1 + \beta_r + [12(1-\nu^2)\alpha_r(1+\alpha_s)\gamma_r^2]/\alpha_0 \qquad \bar{D}_{xy} = 1 + [12(1-\nu^2)\nu\alpha_s\alpha_r\gamma_s\gamma_r]/\alpha_0 \qquad \bar{D}_{yx} = \bar{D}_{xy}$$

$$\bar{H}_{xx} = [1+\alpha_s(1-\nu^2)]/\alpha_0 \qquad \bar{H}_{yy} = [1+\alpha_r(1-\nu^2)]/\alpha_0 \qquad \bar{H}_{xy} = (1+\nu) - \nu/\alpha_0 \qquad \bar{H}_{yx} = \bar{H}_{xy}$$

$$\bar{Q}_{xx} = \nu\alpha_s\gamma_s/\alpha_0 \qquad \bar{Q}_{yy} = \nu\alpha_r\gamma_r/\alpha_0 \qquad \bar{Q}_{xy} = -[\alpha_s\gamma_s\{1+(1-\nu^2)\alpha_r\} + \alpha_r\gamma_r\{1+(1-\nu^2)\alpha_s\}]/2\alpha_0 \qquad \bar{Q}_{yx} = \bar{Q}_{xy}$$

[a] $\frac{a}{E}(D_{xx}, D_{xy}, D_{yy}) = [Et^3/12(1-\nu^2)](\bar{D}_{xx}, \bar{D}_{xy}, \bar{D}_{yy})$, $(Q_{xx}, Q_{xy}, Q_{yy}) = t(\bar{Q}_{xx}, \bar{Q}_{xy}, \bar{Q}_{yy})$; $(H_{xx}, H_{xy}, H_{yy}) = (1/Et)(\bar{H}_{xx}, \bar{H}_{xy}, \bar{H}_{yy})$, $(B_{xx}, B_{xy}, B_{yx}, B_{yy}) = Et^2(\bar{B}_{xx}, \bar{B}_{xy}, \bar{B}_{yx}, \bar{B}_{yy})$; $\alpha_s = A_s/d_st$, $\beta_s = EI_s/\bar{D}d_s$, $\gamma_s = e_s/t$; $\alpha_r = A_r/d_rt$, $\beta_r = EI_r/\bar{D}d_r$, $\gamma_r = e_r/t$; $\alpha_0 = (1+\alpha_s)(1+\alpha_r) - \nu^2\alpha_s\alpha_r$.

In the calculations, one or the other of the reference values of the loadings p^0 and P^0 will actually be zero. These prebuckling stresses are not exact since they are obtained on the basis of the usual "classical" assumption that the prebuckling displacements can be neglected. In fact, a simply supported cylinder undergoes a slight barreling or bowing-in depending on whether the loading is axial compression or hydrostatic, and the prebuckling stresses will not be uniform prior to buckling. This effect, which is probably more important for the case of stringer stiffening than ring stiffening, is neglected in this paper. Simple-support boundary conditions, written in terms of the displacement W and the stress function for the additional stresses, are equivalent to

$$F = F_{,xx} = W = W_{,xx} = 0 \qquad \text{at } x = 0, L \tag{21}$$

The postbuckling analysis of the perfect structure proceeds along the lines laid out by Koiter in his general theory of postbuckling analysis.[4-6] This theory will not be redeveloped here. Results, essential to the calculations, have been taken from Refs. 20 and 21, which contain a reworked version of Koiter's theory. We anticipate that the eigenvalue problem for the classical buckling load λ_C will yield a unique buckling mode $W^{(1)}$ with the associated stress function $F^{(1)}$. A solution, to be valid in the initial postbuckling regime, is sought in the form of an asymptotic expansion

$$\begin{aligned} W &= (\delta/t)W^{(1)} + (\delta/t)^2W^{(2)} + \ldots \\ F &= \lambda F^0 + (\delta/t)F^{(1)} + (\delta/t)^2F^{(2)} + \ldots \end{aligned} \tag{22}$$

where $W^{(1)}$ will be normalized such that δ/t is the ratio of the buckling normal displacement amplitude to the shell thickness and $W^{(2)}$ is orthogonal to $W^{(1)}$ in some appropriate sense.

A formal substitution of this expansion into the nonlinear governing equations (15) and (16) generates a sequence of linear equations for the functions appearing in the expansion. The set of equations for $W^{(1)}$ and $F^{(1)}$ comprises the classical eigenvalue problem, i.e.,

$$\begin{aligned} L_D[W^{(1)}] + L_Q[F^{(1)}] - \lambda_C(N_x^0 + N_s^0)W_{,xx}^{(1)} - \\ \lambda_C(N_y^0 + N_r^0)W_{,yy}^{(1)} = 0 \\ L_H[F^{(1)}] - L_Q[W^{(1)}] = 0 \end{aligned} \tag{23}$$

with $W^{(1)} = W_{,xx}^{(1)} = F^{(1)} = F_{,xx}^{(1)} = 0$ at $x = 0, L$. The boundary value problem for $W^{(2)}$ and $F^{(2)}$ comes from the next higher terms in the expansion

$$\begin{aligned} L_D[W^{(2)}] + L_Q[F^{(2)}] - \lambda_C(N_x^0 + N_s^0)W_{,xx}^{(2)} - \\ \lambda_C(N_y^0 + N_r^0)W_{,yy}^{(2)} = F_{,xx}^{(1)}W_{,yy}^{(1)} + \\ F_{,yy}^{(1)}W_{,xx}^{(1)} - 2F_{,xy}^{(1)}W_{,xy}^{(1)} \\ L_H[F^{(2)}] - L_Q[W^{(2)}] = W_{,xy}^{(1)2} - W_{,xx}^{(1)}W_{,yy}^{(1)} \end{aligned} \tag{24}$$

with $W^{(2)} = W_{,xx}^{(2)} = F^{(2)} = F_{,xx}^{(2)} = 0$ at $x = 0, L$.

The buckling deflection δ is related to the load parameter λ in the initial post-buckling regime by the scalar equation

$$\lambda/\lambda_C = 1 + a(\delta/t) + b(\delta/t)^2 + \ldots \tag{25}$$

General expressions for these postbuckling coefficients applicable to a fairly wide class of theories, in which the present theory is included, are given in Refs. 20 and 21. For the eccentrically stiffened cylinders these expressions reduce to

$$a = \frac{\frac{3}{2}\int_S [F_{,xx}^{(1)}W_{,y}^{(1)2} + F_{,yy}^{(1)}W_{,x}^{(1)2} - 2F_{,xy}^{(1)}W_{,x}^{(1)}W_{,y}^{(1)}]dS}{-\lambda_C\int_S [F_{,xx}^{0}W_{,y}^{(1)2} + F_{,yy}^{0}W_{,x}^{(1)2}]dS} \tag{26}$$

$$\begin{aligned} b = \Big\{ & 2\int_S [F_{,xx}^{(1)}W_{,y}^{(1)}W_{,y}^{(2)} + F_{,yy}^{(1)}W_{,x}^{(1)}W_{,x}^{(2)} - \\ & F_{,xy}^{(1)}(W_{,x}^{(1)}W_{,y}^{(2)} + W_{,y}^{(1)}W_{,x}^{(2)})]dS + \\ & \int_S [F_{,xx}^{(2)}W_{,y}^{(1)2} + F_{,yy}^{(2)}W_{,x}^{(1)2} - \\ & 2F_{,xy}^{(2)}W_{,x}^{(1)}W_{,y}^{(1)}]dS\Big\} \div \\ & \Big\{-\lambda_C\int_S [F_{,xx}^{0}W_{,y}^{(1)2} + F_{,yy}^{0}W_{,x}^{(1)2}]dS\Big\} \end{aligned} \tag{27}$$

The classical buckling load is the lowest of all the eigenvalues admitted by Eqs. (23). These can be written compactly as

$$\lambda_{m\bar{n}} = \frac{-1}{2\bar{Z}[(\bar{N}_x^0 + \bar{N}_s^0)m^2 + (\bar{N}_y^0 + \bar{N}_r^0)\bar{n}^2]} \times \left[D_{(m,\bar{n})} + \frac{(2CQ_{(m,\bar{n})} - \bar{Z}m^2)^2}{H_{(m,\bar{n})}}\right] \tag{28}$$

and are associated with the eigenmodes

$$W^{(1)} = t\sin(m\pi x/L)\cos(ny/R) \tag{29}$$

$$F^{(1)} = \frac{Et^3}{2C^2}\bar{F}\sin\frac{m\pi x}{L}\cos\frac{ny}{R} \qquad \bar{F} = \frac{2C^2Q_{(m,\bar{n})} - C\bar{Z}m^2}{H_{(m,\bar{n})}}$$

where the barred quantities appearing in these expressions are defined in the Nomenclature. In addition, it has been convenient to introduce the abbreviations

$$\begin{aligned} D_{(\alpha,\beta)} &= \bar{D}_{xx}\alpha^4 + 2\bar{D}_{xy}\alpha^2\beta^2 + \bar{D}_{yy}\beta^4 \\ Q_{(\alpha,\beta)} &= \bar{Q}_{xx}\alpha^4 + 2\bar{Q}_{xy}\alpha^2\beta^2 + \bar{Q}_{yy}\beta^4 \\ H_{(\alpha,\beta)} &= \bar{H}_{xx}\alpha^4 + 2\bar{H}_{xy}\alpha^2\beta^2 + \bar{H}_{yy}\beta^4 \end{aligned} \tag{30}$$

All classical buckling loads presented in this paper were obtained by minimizing $\lambda_{m\bar{n}}$ with respect to integer values of m and continuously with respect to $\bar{n} = nL/\pi R$. Of course, quantitative application of Donnell-type theory is restricted to values of n greater than five, say, except when the shells buckle axisymmetrically in which case the theory is also valid. One can show that Eq. (28) is the same as the corresponding expression for the case of zero torsional and lateral stiffnesses in Ref. 7.

At this point, it is readily verified that the first postbuckling coefficient a is identically zero and, therefore, it is necessary to solve for $W^{(2)}$ and $F^{(2)}$ in order to calculate b [see Eq. (27)]. The right-hand side of Eqs. (24) involve the known functions $W^{(1)}$ and $F^{(1)}$ in such a way that one can seek sepa-

rated solutions of the form

$$W^{(2)} = t\left(\sum_{i=1}^{\infty} \alpha_i \sin\frac{i\pi x}{L} + \cos\frac{2ny}{R}\sum_{i=1}^{\infty} \gamma_i \sin\frac{i\pi x}{L}\right)$$
$$F^{(2)} = \frac{Et^2}{2C^2}\left(\sum_{i=1}^{\infty} \beta_i \sin\frac{i\pi x}{L} + \cos\frac{2ny}{R}\sum_{i=1}^{\infty} \zeta_i \sin\frac{i\pi x}{L}\right) \quad (31)$$

Each individual term of these series satisfies all the boundary conditions and the coefficients are easily determined by the Galerkin procedure. They are

$$\left.\begin{aligned}
\alpha_i &= -[8m^2\bar{n}^2/\pi i(i^2 - 4m^2)\rho_i] \times \\
&\qquad [\bar{F}\bar{H}_{xx}i^2 + C^2\bar{Q}_{xx}i^2 - \tfrac{1}{2}C\bar{Z}] \\
\beta_i &= [8m^2\bar{n}^2/\pi i(i^2 - 4m^2)\rho_i]\{\bar{F}(2C^2\bar{Q}_{xx}i^2 - \bar{Z}C) - \\
&\qquad (C^2/2)[\bar{D}_{xx}i^2 + 2\bar{Z}\lambda_C(\bar{N}_x{}^0 + \bar{N}_s{}^0)]\} \\
\gamma_i &= -(8m^2\bar{n}^2/\pi i\phi_i)[\bar{F}H_{(i,\,2\bar{n})} + C^2Q_{(i,\,2\bar{n})} - \tfrac{1}{2}C\bar{Z}i^2] \\
\zeta_i &= -(8m^2\bar{n}^2/\pi i\phi_i)[\bar{F}(2C^2Q_{(i,\,2\bar{n})} - C\bar{Z}i^2) - \\
&\qquad (C^2/2)(D_{(i,\,2\bar{n})}) + 2\bar{Z}\lambda_C(\bar{N}_x{}^0 + \bar{N}_s{}^0)i^2 + \\
&\qquad 8\bar{Z}\lambda_C(\bar{N}_y{}^0 + \bar{N}_r{}^0)\bar{n}^2]
\end{aligned}\right\} \quad (32)$$

for $i = 1, 3, 5 \ldots$, and zero if i is even and where

$$\rho_i = \bar{D}_{xx}\bar{H}_{xx}i^4 + (2C\bar{Q}_{xx}i^2 - \bar{Z})^2 + 2\bar{Z}\lambda_C(\bar{N}_x{}^0 + \bar{N}_s{}^0)\bar{H}_{xx}i^2$$
$$\phi_i = H_{(i,\,2\bar{n})}[D_{(i,\,2\bar{n})} + 2\bar{Z}\lambda_C(\bar{N}_x{}^0 + \bar{N}_s{}^0)i^2 + 8\bar{Z}\bar{n}^2\lambda_C(\bar{N}_y{}^0 + \bar{N}_r{}^0)] + [2CQ_{(i,\,2\bar{n})} - \bar{Z}i^2]^2$$

It also can be shown that the conditions for single-valued tangential displacements are satisfied up to and including terms of order $(\delta/t)^2$.

Now, it only remains to calculate the postbuckling coefficient b. This is accomplished in a straightforward way using Eq. (27) and the series expressions listed previously. One finds

$$b = \frac{-4m^2\bar{n}^2}{\pi\bar{Z}\lambda_C[(\bar{N}_x{}^0 + \bar{N}_s{}^0)m^2 + (\bar{N}_y{}^0 + \bar{N}_r{}^0)\bar{n}^2]} \times \left[2\sum_i \frac{i(2\bar{F}\alpha_i + \beta_i)}{(i^2 - 4m^2)} + \sum_i (2\bar{F}\gamma_i + \zeta_i)\frac{1}{i}\right] \quad (33)$$

This series representation was evaluated numerically by terminating the series after a sufficient number of terms had been included to insure a truncation error of less than one tenth of one percent. All calculations, for the classical buckling loads and the postbuckling coefficient, were made with Poisson's ratio equal to $\frac{1}{3}$.

From the Koiter analysis, it follows that an imperfection in the form of the buckling mode

$$\bar{W} = \bar{\delta}\sin(m\pi x/L)\cos(ny/R)$$

results in the following modification of the relation of load to buckling deflection in the initial postbuckling regime:

$$\left(1 - \frac{\lambda}{\lambda_C}\right)\left(\frac{\delta}{t}\right) + b\left(\frac{\delta}{t}\right)^3 = \frac{\lambda}{\lambda_C}\left(\frac{\bar{\delta}}{t}\right) \quad (34)$$

The buckling load of the imperfect structure λ_S is found by maximizing λ with respect to δ, which leads directly to Eq. (2) from which the curves of λ_S/λ_C vs $\bar{\delta}/t$ of Fig. 1 were obtained.

Buckling in the Presence of Axisymmetric Imperfections

Under certain conditions it is found that the classical buckling mode is axisymmetric and, when it is, b is identically zero. A different method of analysis is clearly called for if one is to assess to what extent, if any, imperfections reduce the buckling load. The method that has been employed in this paper is similar in most respects to that used by Koiter[16] to study the effect of axisymmetric imperfections on buckling of unstiffened cylinders under axial compression. Only a brief description of the analysis will be given here.

First, consider a cylinder with outside axial stiffening under axial load. As discussed in the body of the paper, this shell buckles axisymmetrically for all Z below a certain value. If an imperfection in the shape of the buckling mode is assumed,

$$\bar{W} = -\bar{\delta}\sin(\pi x/L) \quad (35)$$

the governing nonlinear equations (15) and (16) admit a relatively simple axisymmetric prebuckling solution (as in the classical and postbuckling calculations, the prebuckling displacement associated with the perfect cylinder is neglected). The total displacement and stress function can be written as

$$W = W_a + w \qquad F = F_a + f \quad (36)$$

where W_a and F_a, which are functions of P, $\bar{\delta}$, and x, comprise the prebuckling solution; and w and f are nonzero only after bifurcation from the axisymmetric state has taken place. A linear eigenvalue problem for the bifurcation load P_S is obtained if W and F are substituted into the governing equations and if, then, these equations are linearized with respect to w and f. Two variable coefficient equations result:

$$L_D[w] + L_Q[f] = F_{a,\,xx}w_{,yy} + f_{,yy}W_{a,\,xx} \quad (37)$$
$$L_H[f] - L_Q[w] = -W_{a,\,xx}w_{,yy} \quad (38)$$

with $w = w_{,xx} = f = f_{,xx} = 0$ at $x = 0, L$. Any eigenmode could be written in the form

$$w = \cos\frac{ny}{R}\sum_i a_i \sin\frac{i\pi x}{L}$$

The curves presented in Fig. 4 were based on an approximate calculation in which only the first term in the preceding sine series was retained. Equation (38) was solved exactly for f in terms of the assumed w and then the Galerkin procedure was applied to Eq. (37) to obtain an eigenvalue equation for P_S in terms of $\bar{\delta}$ and $\bar{n} = nL/\pi R$. For a given imperfection magnitude $\bar{\delta}$, P_S is minimized with respect to $\bar{n}$. This step was performed numerically. As discussed in Ref. 16, this procedure leads to an upper bound estimate of P_S.

The same approach was used to determine the effect of the axisymmetric imperfection

$$\bar{W} = \bar{\delta}\sin(2\pi x/l)$$

on the buckling load of axially compressed and hydrostatically loaded cylinders. In this instance the analysis is appropriate for cylinders whose length L is long compared to the imperfection wave length l [see Eq. (9)]. Again, an axisymmetric prebuckling solution is easily produced and the eigenvalue problem for the bifurcation load is in the form of Eqs. (37) and (38). An approximate nonaxisymmetric mode is assumed

$$w = \sin\pi(x/l + \tfrac{3}{4})\cos(ny/R)$$

and the eigenvalue equation for the bifurcation load or pressure is obtained. This displacement w will not satisfy the simple-support end condition at $x = 0$ and L but this makes little difference as long as the cylinder length is several times the wavelength l. Results of these calculations have been presented in Figs. 7 and 10. The upper bound curve for the unstiffened cylinder, shown in Fig. 7 and orginally obtained by Koiter,[16] also is retrieved from the present calculations.

References

[1] van der Neut, A., "General instability of stiffened cylindrical shells under axial compression," National Luchtvaartlaboratorium, Holland, Vol. 13, Rept. S 314 (1947).

[2] Hedgepeth, J. M. and Hall, D. B., "Stability of stiffened cylinders," AIAA J. 3, 2275–2286 (1965).

[3] Baruch, M. and Singer, J., "Effect of eccentricity of stiffeners on the general instability of stiffened cylindrical shells under hydrostatic pressure," J. Mech. Eng. Sci. 5, 23 (March 1963).

[4] Koiter, W. T., "On the stability of elastic equilibrium," Thesis, Delft (H. J. Paris, Amsterdam, Holland, 1945), in Dutch.

[5] Koiter, W. T., "Elastic stability and post-buckling behavior," *Non-Linear Problems*, edited by R. E. Langer (University of Wisconsin Press, Madison, Wis., 1963).

[6] Koiter, W. T., "General equations of elastic stability for thin shells," *Donnell Testimonial Meeting*, Houston, Texas, April 1966 (to be published).

[7] Block, D. L., Card, M. F., and Mikulas, M. M., "Buckling of eccentrically stiffened orthotropic cylinders," NASA Langley Research Center TN D-2960 (August 1965).

[8] Singer, J., Baruch, M., and Harari, O., "On the stability of eccentrically stiffened cylindrical shells under axial compression," Technion Research and Development Foundation, Haifa, Israel, TAE Rept. 44 (August 1965).

[9] Crawford, R. F., "Effects of asymmetric stiffening on buckling of shells," AIAA Preprint 65-371 (July 1965).

[10] Card, M. F., "Preliminary results of compression tests on cylinders with eccentric longitudinal stiffeners," NASA Langley Research Center TM X-1004 (September 1964).

[11] Card, M. and Jones, R., "Compressive buckling of cylinders with eccentric longitudinal stiffners," *AIAA/ASME Seventh Structures and Materials Conference* (American Institute of Aeronautics and Astronautics, New York, 1966), pp. 23–27; also NASA Langley Research Center TND-3639.

[12] Almroth, B. O., "Post-buckling behavior of orthotropic cylinders under axial compression," AIAA J. 2, 1795–1799 (1964).

[13] Batdorf, S. B., "A simplified method of elastic-stability analysis for thin cylindrical shells," NACA Langley Research Center Rept. 874 (1947); formerly in NACA Langley Research Center TN 1341.

[14] Budiansky, B. and Amazigo, J. C., "Initial post-buckling behavior of cylindrical shells under external pressure" (to be published).

[15] Dow, D. A., "Buckling and post-buckling tests of ring-stiffened cylinders loaded by uniform external pressure," NASA Langley Research Center TN D-3111 (November 1965).

[16] Koiter, W. T., "The effect of axisymmetric imperfections on the buckling of cylindrical shells under axial compression," Koninkl. Ned. Akad. Weterschap. Proc. B66, 265–279 (1963).

[17] Thielemann, W. F., "New developments in the nonlinear theories of the buckling of thin cylindrical shells," *Aeronautics and Astronautics, Proceedings of Durand Centennial Conference* (Pergamon Press Ltd., Oxford, 1960), p. 76.

[18] Singer, J., Baruch, M., and Harari, O., "Further remarks on the effects of eccentricity of stiffeners on the general instability of stiffened cylindrical shells," Technion Research and Development Foundation, Haifa, Israel, revised TAE Rept. 42 (August 1965).

[19] Geier, B., "Das Beulverhalten versteifter Zylinderschalen. Teil 1, Differentialgleichungen," Z. Flugwiss. 14, 306 (July 1966).

[20] Budiansky, B. and Hutchinson, J. W., "Dynamic buckling of imperfection-sensitive structures," *Proceedings of the XI International Congress of Applied Mechanics*, edited by H. Görtler (Julius Springer-Verlag, Berlin, 1964), pp. 636–651.

[21] Budiansky, B., "Dynamic buckling of elastic structures: Criteria and estimates," *Proceedings, International Conference on Dynamic Stability of Structures* (Pergamon Press Inc., New York, 1966).